Nano Research 2016, 9(1): 47–58
DOI 10.1007/s12274-015-0970-0
Review Article
ISSN 1998-0124
CN 11-5974/O4

Cooperative effects at the interface of nanocrystalline metal–organic frameworks

Bunyarat Rungtaweevoranit (✉), Yingbo Zhao (✉), Kyung Min Choi, and Omar M. Yaghi (✉)

Department of Chemistry, University of California-Berkeley; Materials Sciences Division, Lawrence Berkeley National Laboratory; Kavli Energy NanoSciences Institute at Berkeley, Berkeley, California 94720, USA

Received: 27 October 2015
Revised: 2 December 2015
Accepted: 6 December 2015

KEYWORDS
metal–organic framework, inorganic nanocrystal, cooperative effects, interface design

ABSTRACT

Controlling the chemistry at the interface of nanocrystalline solids has been a challenge and an important goal to realize desired properties. Integrating two different types of materials has the potential to yield new functions resulting from cooperative effects between the two constituents. Metal–organic frameworks (MOFs) are unique in that they are constructed by linking inorganic units with organic linkers where the building units can be varied nearly at will. This flexibility has made MOFs ideal materials for the design of functional entities at interfaces and hence allowing control of properties. This review highlights the strategies employed to access synergistic functionality at the interface of nanocrystalline MOFs (nMOFs) and inorganic nanocrystals (NCs).

1 Introduction

The synthesis of nanocrystalline metal–organic frameworks (nMOFs) has greatly enriched the library of synthetic nanomaterials. MOFs are versatile functional entities that can be integrated with inorganic nanocrystals (NCs) to build complex mesoscopic constructs, in which the MOF component is composed of covalently linked organic and inorganic units, and imparts porosity and crystallinity to the entire construct [1, 2]. Synergistic effects arising from this integration opens up new opportunities for the design of functional nanomaterials. In this review, we discuss three aspects: the synthesis of nMOFs, the integration of nMOFs and NCs, and the synergistic effects arising from their combination.

2 Synthetic strategies for the preparation of nMOFs

Scaling down the size of MOFs to the nanoregime provides for better diffusion kinetics of guest molecules and processing ability for device fabrication [3, 4]. Furthermore, the preparation methods for nMOFs provide a toolbox for the designer to interface nMOFs with other classes of nanomaterials to engender

Address correspondence to Bunyarat Rungtaweevoranit, bunyaratr@berkeley.edu; Yingbo Zhao, zhaoyybb@berkeley.edu; Omar M. Yaghi, yaghi@berkeley.edu

synergistic effects. We briefly highlight the approaches to prepare MOFs at the nanoscale with special emphasis given in the context of interface design [5–7].

2.1 Coordination modulation

Nanocrystalline materials are prepared by controlling the nucleation and growth of crystals. In carboxylate-based MOFs, the coordination modulation has been particularly useful to control their size and morphology. This approach involves the use of modulator, which is typically a monodentate ligand of the same link functionality as the organic linker used in the synthesis of MOFs. This method relies on organic linkers and modulators competing for the coordination to metal ion in order to regulate the nucleation and growth.

An early example employing this approach to prepare nMOFs was reported in 2007 [8]. In this case, nMOF-5 [$Zn_4O(BDC)_3$; BDC^{2-} = 1,4-benzenedicarboxylate] was synthesized by using *p*-perfluoromethylbenzoic acid as a modulator. Depending on the amount of modulator added, the particle size of nMOF-5 could be tuned between 100 and 150 nm. Note that the obtained material exhibited similar crystallinity as bulk MOF-5. This coordination modulation approach has been further applied to synthesize nMOFs with anisotropic morphology. Here, a MOF {$Cu_2(NDC)_2(DABCO)$, NDC^{2-} = 1,4-naphthalenedicarboxylate; DABCO = 1,4-diazabicyclo[2.2.2]octane} was constructed from two different kinds of connection, i.e., carboxylate-metal bonds within the layer and metal-amine bonds between the layers, and by using acetic acid as a modulator, the growth in the [100] direction which occurs through carboxylate-metal bond formation was suppressed resulting in the production of nanorod forms [9]. The coordination modulation has been proven to be applicable to obtaining other nMOFs with different sizes and morphologies: nHKUST-1 [$Cu_3(BTC)_2$; BTC^{3-} = benzene-1,3,5-tricarboxylate; micron size; cubic, cuboctahedral and octahedral shape] [10], nUiO-66 [$Zr_6(OH)_4O_4(BDC)_6$; 100–500 nm in size; octahedral shape] [11–12] (Fig. 1(a)), nMOF-801 [$Zr_6(OH)_4O_4$(fumarate)$_6$; <200 nm in size; octahedral shape] [13] and nZIF-8 [$Zn(mIM)_2$; mIM = 2-methylimidazolate; 20 nm–1 μm, dodecahedral shape] [14].

2.2 Surfactant additives

Similar to the practice in colloidal synthesis of metal nanocrystals, the use of surfactants is useful to control the size and growth of nMOFs. Surfactants such as cetrimonium bromide (CTAB) have been employed to prepare nHKUST-1 (Fig. 1(b)). Depending on the concentration of CTAB, the morphology can be tuned from cubic to octahedral shapes as the growth rate of {111} facet is regulated by the surfactant [15]. Poly(diallyldimethylammonium chloride) was used as a surfactant to prepare dodecahedral nZIF-8 with 50 nm size [16]. Similarly, polyacrylic acid was employed to prepare nHKUST-1 (30–300 nm in size) [17].

2.3 Localized metal precursor methods

Another strategy to prepare nMOFs uses localized metal precursors, where metal oxide precursors

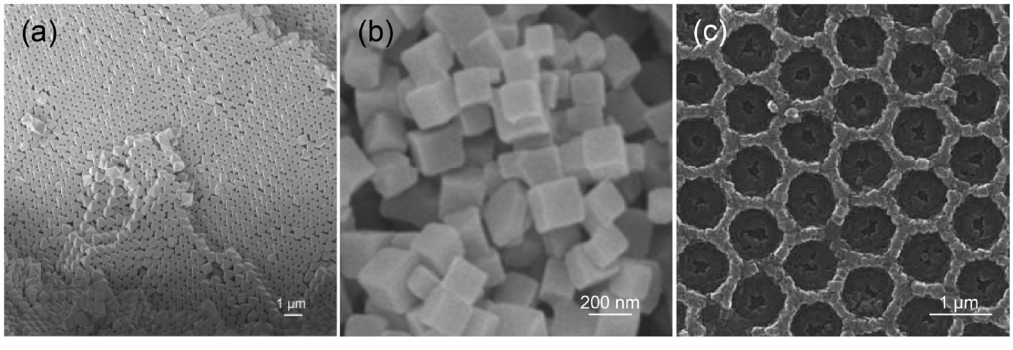

Figure 1 Scanning electron microscopy (SEM) images of monodispersed nUiO-66 (~400 nm in size) obtained by using acetic acid as a modulator (a), cubic nHKUST-1 prepared by using CTAB to control its morphology (b) and [Al(OH)(NDC)] as honeycomb array synthesized by using alumina as a metal oxide template (c). (Adapted with permission from Ref. [12], © John Wiley & Sons, Inc.; Ref. [15], © Royal Society of Chemistry; and Ref. [18], © Nature Publishing Group.)

deposited on substrates gradually dissolve and react with the organic linker at the solid–liquid interface. Such controlled dissolution of metal precursor and the subsequent reaction with the organic linker produce nMOFs whose spatial arrangement is the replica of the original metal oxide template. In 2012, an aluminum oxide template was prepared as a two-dimensional honeycomb pattern and as a three-dimensional inverse opal structure, and converted into [Al(OH)(NDC)] (Fig. 1(c)). Aluminum oxide serves as a template to produce aluminum nMOF with the same pattern as the metal oxide template [18]. An array of nanowire of ZIF-8 was produced by a similar manner using ZnO nanowires as the Zn^{2+} precursor [19]. Atomic layer deposition (ALD) has also been used to produce amorphous aluminum oxide on silver nanocrystals. Here, the aluminum oxide was then allowed to react with porphyrin linkers to produce [$Al_2(OH)_2$TCPP; $TCPP^{4-}$ = 4,4′,4″,4‴-(porphyrin-5,10,15,20-tetrayl)tetrabenzoate]. The thickness of nMOFs can be controlled at the nanoscale depending on the thickness of metal oxide deposited on the substrate [20].

3 Combining nMOFs and inorganic NCs to make mesoscopic constructs

Combining inorganic NCs and nMOFs into one construct has the potential to endow the resulting material with new properties, which the individual components alone may not have. These mesoscopic constructs are fascinating since they juxtapose matter at the atomic level where the nMOFs and NCs are of different size-regime, metric properties, composition, and spatial arrangement. Thus, in the present case, one can view these constructs as being distinct compartments that are linked but may function differently. The interface within this construct can be well-defined by virtue of the high crystallinity of nMOF. Reviews have appeared concerning the preparation of these materials [21–25], thus we briefly describe recent progress in this area.

3.1 Impregnation of metal precursors

One of the earliest methods to introduce metal nanocrystals into MOFs is by using the ship-in-a-bottle approach. Here, MOFs are synthesized and impregnated with metal precursors. Subsequent reduction either by a hydride reducing agent or hydrogen gas yields metal NCs immobilized in MOFs (Fig. 2). As an example, Pd precursor [(η_5-C_5H_5)Pd(η_3-C_3H_5)] was introduced into the pores of MOF-5 by chemical vapor deposition. The adsorbed Pd complex was then treated with H_2 gas to produce Pd NCs. Other metal NCs such as Cu and Au were also prepared by this method [26]. To successfully employ the ship-in-a-bottle approach, several parameters including the interaction between MOF host and metal precursors, the cavity size and the loading of metal precursors should be considered to achieve the control over the size and location of the subsequently formed NCs.

Without such controls, metal NCs were often found as large particles either adsorbed on the surface of the MOF or occupying multiple pores. It has been shown that the interaction between the MOF host and metal precursors could be enhanced by the incorporation of chelating units within the pores. In 2008, the open metal sites of MIL-101 [Cr_3(F,OH)(H_2O)$_2$O(BDC)$_3$] were postsynthetically functionalized with ethylenediamine where its protonated form was employed to localize the metal complex anions, $[PdCl_4]^{2-}$, $[PtCl_6]^{2-}$, and $[AuCl_4]^-$ through columbic interaction. Reduction of these metal complexes with $NaBH_4$ thus produced 2–4 nm Pd NCs homogeneously dispersed in MIL-101 [27]. The presynthesized Pd-complexed-organic linker has also been used to precisely localize the metal precursors to produce Pd in UiO-67 [$Zr_6O_4(OH)_4$(BPDC)$_{6-x}$(BPyDC)$_x$; BPDC = biphenyl-4,4′-dicarboxylate; $BPyDC^{2-}$ = 2,2-bipyridine-5,5′-dicarboxylate] [28]. Double solvents method has been demonstrated as another approach to produce metal NCs in the MOF pores [29]. This approach relies on the hydrophilic interaction of hydrophilic solvent containing metal precursor and hydrophilic MOF pores. Large amount of hydrophobic solvent was used in combination with hydrophilic solvent to drive the confinement of metal precursor in the MOF pores. This procedure provided small Pt NCs in the range of 1.2–3.0 nm immobilized in MIL-101. It should be noted that this double solvents approach could be used for the preparation of bimetallic NCs such as AuNi NCs (Fig. 2(a)) [30] and AuPd NCs [31].

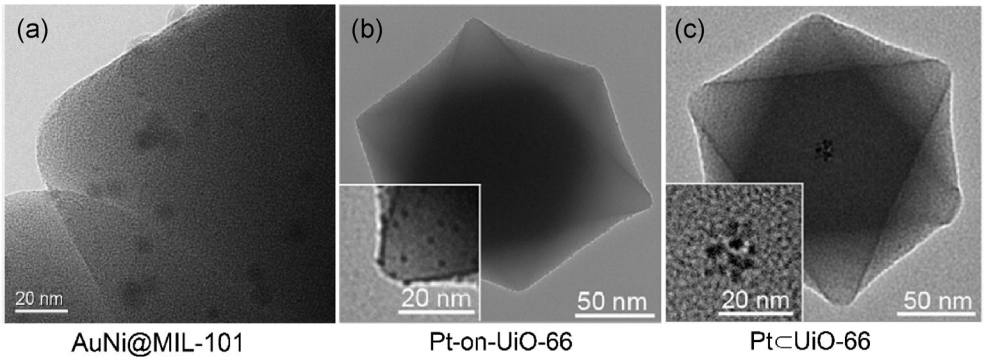

Figure 2 Transmission electron microscope (TEM) images of inorganic NCs incorporated in nMOFs: (a) AuNi@MIL-101 synthesized via the reduction of impregnated metal precursor inside the MOF host, (b) Pt-on-UiO-66 which could be prepared by the physical mixing of Pt NCs and UiO-66, and (c) Pt⊂UiO-66 prepared by the addition of preformed Pt NCs to the solution of UiO-66 precursors. (Adapted with permissions from Refs. [30, 36], © American Chemical Society 2013–2014.)

3.2 Encapsulation of metal NCs in nMOFs

Although the impregnation of metal precursors followed by reduction approach has shown interesting properties, some challenges still exist concerning the control of metal nanomaterials' size, morphology, composition, location, and order. This is important as these features largely determine the properties of nanomaterials in most applications. A second approach has been recently developed to express better control over the design of the mesoscopic construct. Here, the metal NCs are synthesized with the desired metrics and then encapsulated into the nMOFs [22, 32–41]. The common synthetic approach to realize this is to synthesize nMOFs in the presence of NCs with proper interactions between them [22, 33, 36, 39, 40]. Choosing the proper capping agents to provide strong interactions with MOF crystal nuclei, and disperse the NCs during MOF synthesis induces the heterogeneous nucleation of MOF on the surface of NCs. At the same time, the MOF synthetic conditions should be controlled to suppress homogeneous nucleation by varying the amount of modulator, concentration of linker and metal precursor, temperature, and reaction time.

A general method for encapsulation was introduced in 2012 [39]: The synthesis was demonstrated for various NCs, such as Pt, CdTe, Fe_3O_4 and lanthanide-doped $NaYF_4$ NCs, Ag nanocubes, polystyrene nanospheres, β-FeOOH nanorods and lanthanide-doped $NaYF_4$ nanorods, encapsulated by nZIF-8. The surface of nanoparticles was functionalized with polyvinylpyrrolidone (PVP), which not only maintains the colloidal stability of the NCs but also increases their interactions with ZIF-8, and then introduced into the synthesis solution of ZIF-8 at different time in order to control the position of metal NCs in ZIF-8. Recently, polydopamine has been reported to give better interaction with MOFs, stability of metal NCs, and nucleation sites for both MOFs and NCs [32]. Changing the linkers, metal precursors, and synthetic conditions in the presence of surface-functionalized NCs further diversifies the structure of MOFs encapsulating NCs. Thus, a variety of nMOFs of multiple organic units and metal ions, discrete and infinite metal oxide units, and a variety of structure types have been used and reported between 2011 and 2014 [34, 35, 37, 38, 41].

The control of the position of Pt NCs inside or outside of nMOFs was reported where their size and morphology was precisely controlled (Figs. 2(b) and 2(c)) [36]. In 2015, it was demonstrated that the physical and chemical properties of nMOFs encapsulating Pt NCs can be controlled by varying functionalities on the organic linkers [33].

3.3 Spatial control of NCs encapsulated in nMOFs

In order to further exploit the properties achieved by the integration of nMOF and inorganic NCs, progressively well-defined mesoscopic constructs are being pursued [20, 34, 37, 38, 40, 42]. Employing surfactant (PVP) and carefully choosing the solvents, noble metal NCs enclosed by nMOFs can be prepared by having the NCs generated *in-situ* and individually enclosed in the nMOF (Figs. 3(a) and 3(b)) [38]. This

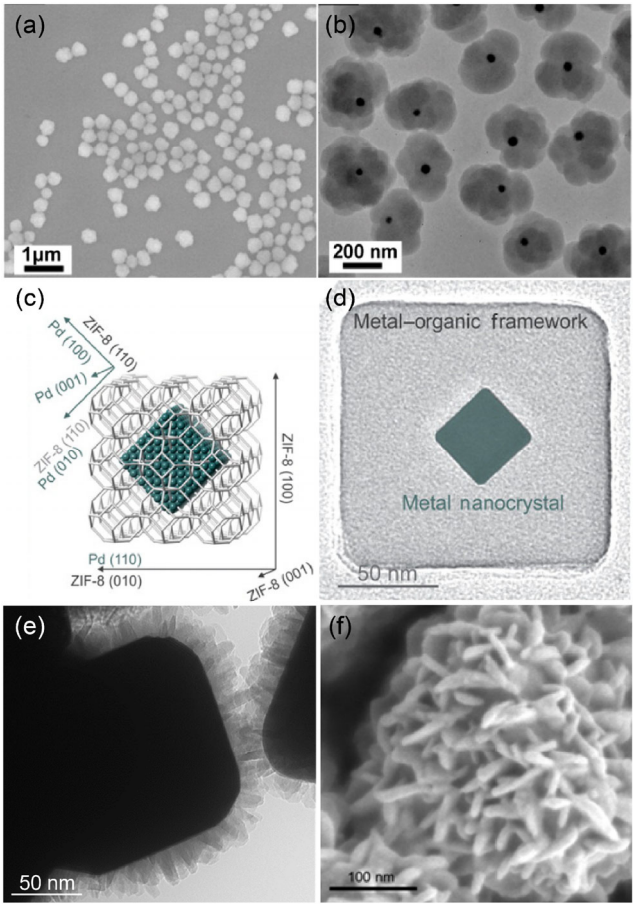

Figure 3 Constructs beyond simple encapsulation of NCs in MOFs: core–shell structures where single NC is enclosed in single MOF ((a) and (b)); single crystalline NC in single crystalline MOF where the relative orientation of the NC and MOF is controlled ((c) and (d)); oriented MOF enclosure on surfactant free silver NC ((e) and (f)). (Adapted with permissions from Refs. [20, 34, 37], © American Chemical Society 2014–2015.)

approach gives rise to stable colloids, well-defined nano objects that show cascade catalytic properties [34]. The amount of surfactant added, as well as the reaction time, can be tuned to control the thickness of the nMOF enclosure. The other approach to produce similar structures is to use metal oxide as a localized metal source. By reacting alumina coated gold nanorods with 1,4-naphthalenedicarboxylic acid at 180 °C and pH 2 water, the corresponding nMOF shell can be deposited on single gold nanorod [42].

The next milestone in the synthetic development of mesoscopic constructs is the control of relative orientation of the MOF to the NC. As to the surfactant directed growth, surfactant molecules adsorb on the surface of the inorganic NC to form a layer, onto which the MOF grows in an oriented fashion. In 2014, it was demonstrated that single NC can be encapsulated individually in single-crystalline nZIF-8 with a specific alignment between the {100} planes of the metal and {110} planes of the ZIF (Figs. 3(c) and 3(d)) [37]. As to the localized metal source approach, although no surfactant is needed, the MOF enclosure can have a specific orientation on NCs, which was readily observed with $Al_2(OH)_2TCPP$ type MOFs grown on 300 nm surfactant free silver octahedral using alumina as localized metal source (Figs. 3(e) and 3(f)) [20].

4 Synergistic effects arising from integration of inorganic NCs and nMOF

4.1 Plasmonic effects

Surface plasmon, the collective oscillation of electrons on metal interfaces stimulated by light, gives an intense electronic field that typically penetrates several nanometers into the media surrounding the metal NC. This electronic field enables SERS (surface-enhanced Raman spectroscopy), which gives chemical information (vibrational bands) of species spatially positioned near the metal NC. With noble metal NCs, such as silver and gold, encapsulated in nMOFs, the chemical characteristics of the MOF, as well as the guest in the pores, can be probed [20, 38, 43]. For example gold NCs encapsulated in $Zn_4O(BPDC)_3$ gives SERS signals, thus reporting the solvent into which this mesoscopic construct is dispersed [44]. As MOFs have substrate selectivity, certain species can be more favorably absorbed into MOFs, thus being detected preferentially by SERS, as exemplified by CO/N_2 in silver encapsulated MOF-5 NCs [38]. Other examples include nZIF-8 coated on silver NCs which is found to trap organic molecules, such as benzene, that otherwise would not adsorb on silver surface, thus enabling the detection of such molecules by SERS (Figs. 4(a) and 4(b)) [43]. More elaborate systems, such as the 2D assembly of MOF enclosed silver NC, provides a platform where chemical information encoded in multivariate MOFs can be mapped by SERS [20]. In this case, unmetallated and metallated porphyrins are incorporated in $Al_2(OH)_2TCPP\text{-}X$ (X = Co, H_2) MOF that enclose the silver NCs. These mesoscopic constructs are packed

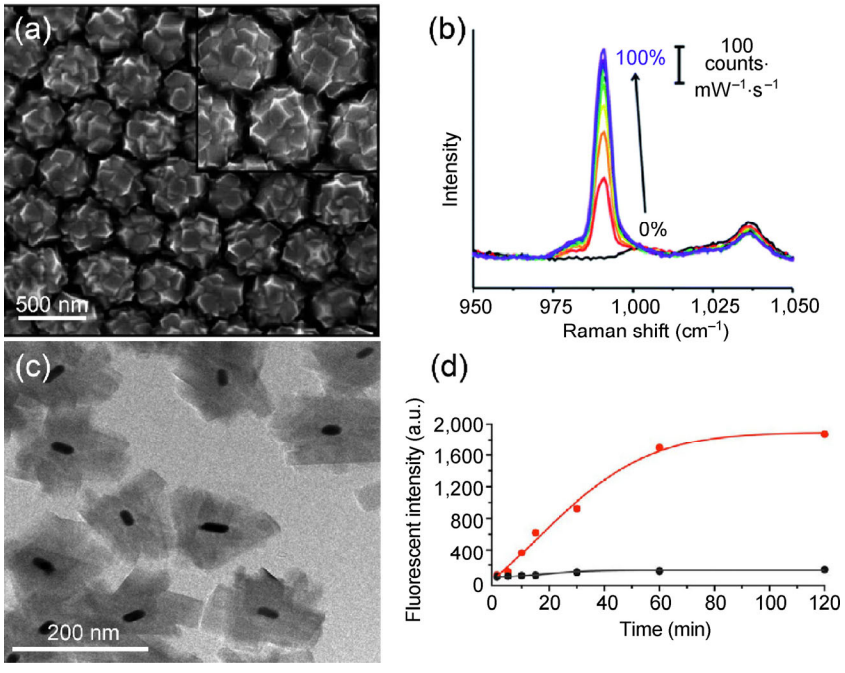

Figure 4 The plasmonic NCs interact synergistically with MOFs. ZIF-8 enclosure of silver coated nanosphere (a) can be used to detect molecules (i.e., benzene) that does not absorb on bare silver surface, as benzene molecules absorbed by the MOF can be detected by SERS enabled by silver coated nanosphere. Vibration band of benzene in the Raman spectra increases with benzene vapor loading (b). The gold nanorod in Al(OH)(NDC) (c) can be used to heat up the MOF upon light irradiation and release the anthracene molecules loaded in the MOF (d). The anthracene loaded MOF-NC construct is dispersed in cyclohexane, the fluoresce of which is monitored. With near infrared light irradiation (red curve), the anthracene is released into the cyclohexane to show fluorescence while without light the fluorescence of the supernatant remains at low level. (Adapted with permissions from Ref. [42], © American Chemical Society; Ref. [43], © Royal Society of Chemistry.)

in monolayer, and confocal SERS mapping reads out the relative ratio of the metallated and unmetallated linkers on each of the silver nanocrystals (300 nm in size) and reveals a homogenous distribution of the two linkers on this length scale.

Surface plasmon, stimulated by light, converts the energy of incoming photon into heat. Thus metal NCs embedded in MOFs can be used as "hot spot" once irradiated and heat up the surrounding MOFs to release the guest molecules absorbed within their interior [42]. Gold nanorods encapsulated Al(OH)(NDC) crystals with drug molecules in their pores can release these drug molecules upon light irradiation (Figs. 4(c) and 4(d)). This construct is a stimuli responsive platform that enables controlled drug release using MOFs.

4.2 Steric and size selective effects

nMOFs encapsulating inorganic nanostructures, with their well-defined pore dimensions, provide diffusion barrier that only allows molecules below certain size to access the enclosed objects. This size selectivity of the MOF enclosures, combined with the catalytic properties of the inorganic core, give rise to unique catalytic properties. In the case of ZIF-ZnO mesoscopic structure (Fig. 5(a)), the ZnO nanorods are reacted with 2-methylimidazole to create a ZIF-8 shell enclosing the ZnO rods [19]. The semiconducting ZnO nanorods generate electron–hole pairs upon photo-illumination, with the hole being scavenged by molecular species, H_2O_2 and ascorbic acid, and electron transferred to the electrode (photoelectrochemistry). H_2O_2 and ascorbic acid behave similarly on ZnO surface, but when ZIF-8 is coated, the ascorbic acid becomes too large to pass through the pores of ZIF-8 shell and participate in the photoelectrochemistry reaction. This photoelectrode proved applicable as H_2O_2 sensor in buffer solutions.

This substrate selectivity of MOF plays an important role in catalyst design, where a more complex

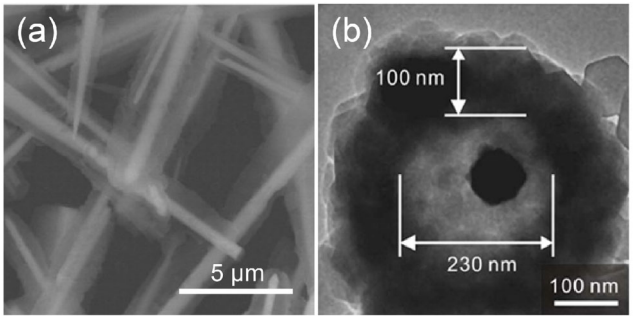

Figure 5 Inorganic nanomaterials integrated with MOFs show size selective catalytic properties and demonstrate the steric effects of the MOF enclosure. ZIF-8 enclosure on ZnO nanorods (a) allows H_2O_2 but not ascorbic acid to access the ZnO electrode. Yolk–shell ZIF-8 enclosed Pd NC (b) shows different activation energy compared to core–shell Pd-ZIF-8 constructs (Pd NCs directly enclosed by ZIF-8 without cavity between them). (Adapted with permission from Refs. [19, 40], © American Chemical Society 2012–2013.)

synergistic effect between MOF and the NC is observed. Palladium catalyzed alkene hydrogenation is used as a model reaction to compare the catalytic properties of Pd NCs, Pd-ZIF-8 mesoscopic structures, Pd-ZIF-8 yolk–shell structures (Fig. 5(b)) [40]. In the case of the yolk–shell structure, 80 nm Pd nanocrystals are enclosed by ZIF-8 shell with 100 nm thickness and 230 nm internal diameter, leaving tens of nanometer void space between the ZIF and the Pd NC. Ethylene molecules react similarly on the three different catalysts, while cyclooctene can only be hydrogenated on Pd NC, being too large to get through the ZIF-shell. Interestingly, the cyclohexene molecules can react on all three catalysts, but the activation energy of the reaction on core–shell catalyst is different from that of the yolk–shell structure and Pd NC only. This result indicates the potential of MOF-metal NC interface in influencing the reaction mechanism.

4.3 Chemical environment control

Catalytic performance of metal NCs is largely controlled by structure and properties at the catalyst surface. This includes the size, composition, and morphology of metal NCs and their exterior. In comparison to other factors, the exteriors of metal NCs are generally ill defined and hence difficult to study and control the catalytic properties. MOF coating around metal NCs can provide tunable environment where chemical functionalities can be controlled through MOF chemistry while the main constructs remain unchanged (Fig. 6).

In 2014, the synergistic interplay between metal NCs and MOFs coating were reported [34]. Pd NCs encapsulated in IRMOF-3 [$Zn_4O(BDC\text{-}NH_2)_3$] as a core–shell structure were synthesized and studied for the cascade Knoevenagel reaction followed by hydrogenation of the respective compound (Fig. 7). Pd NCs encapsulated in IRMOF-3 showed higher selectivity towards hydrogenation of NO_2 group rather than alkene as compared to Pd NCs-on-IRMOF-3. This results from the pore confinement and the interaction between amino group on the pore surface and NO_2 on the substrate that dictate the orientation of substrate traversing through the pore where NO_2 were pointing towards Pd surface.

Recently, Pt NCs fully encapsulated within nUiO-66 were prepared and studied for catalytic conversion of methylcyclopentane [33]. In this construct, Pt NCs of the same size and shape were used allowing the systematic study of catalytic activity arising from the change in exterior of NCs. The chemical environment around Pt NCs were systematically controlled by the incorporation of $–NH_2$/$–NH_3^+$ (denoted as nUiO-66-N* and nUiO-66-N), –SOOH/$–SOO^-$ (denoted as nUiO-66-S and nUiO-66-S*) or combination of both functionalities on the organic linker while the framework remains the same (Figs. 8(a) and 8(b)). Pt⊂nUiO-66-S exhibited 62.4% selectivity toward cyclohexane, the highest reported for this reaction while the catalytic activity was enhanced by 2-fold in comparison to Pt-on-SiO_2 and Pt⊂nUiO-66 (Figs. 8(c) and 8(d)). This enhancement has been attributed to the synergistic catalytic interplay

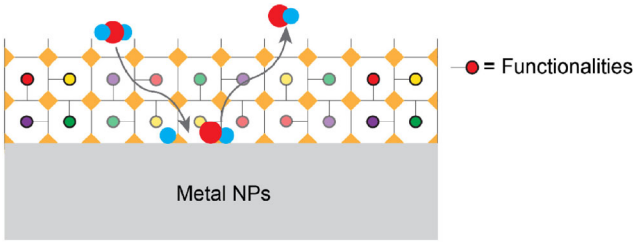

Figure 6 Illustration of chemical environment control of catalytic reactions at the interface of metal NCs and nMOFs where the pore size and functionalities can be fine tuned. Blue and red solid circles represent guest molecules being catalyzed.

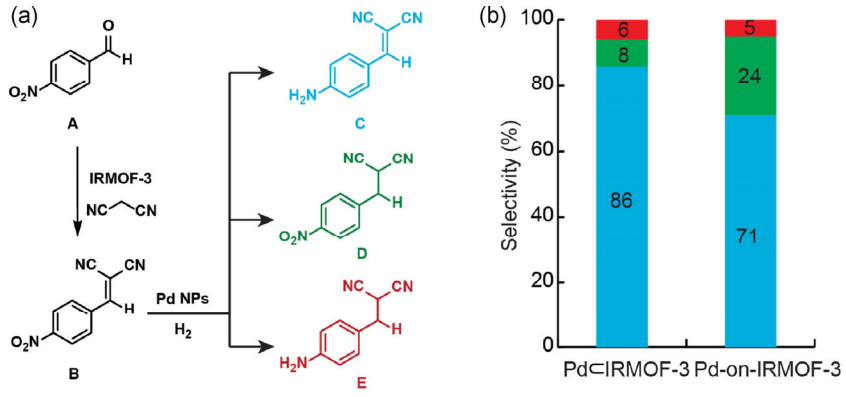

Figure 7 (a) Model cascade Knoevenagel condensation followed by hydrogenation, and (b) change in product selectivity was observed due to the interaction between the MOF pore and substrate that control its orientation during the catalysis.

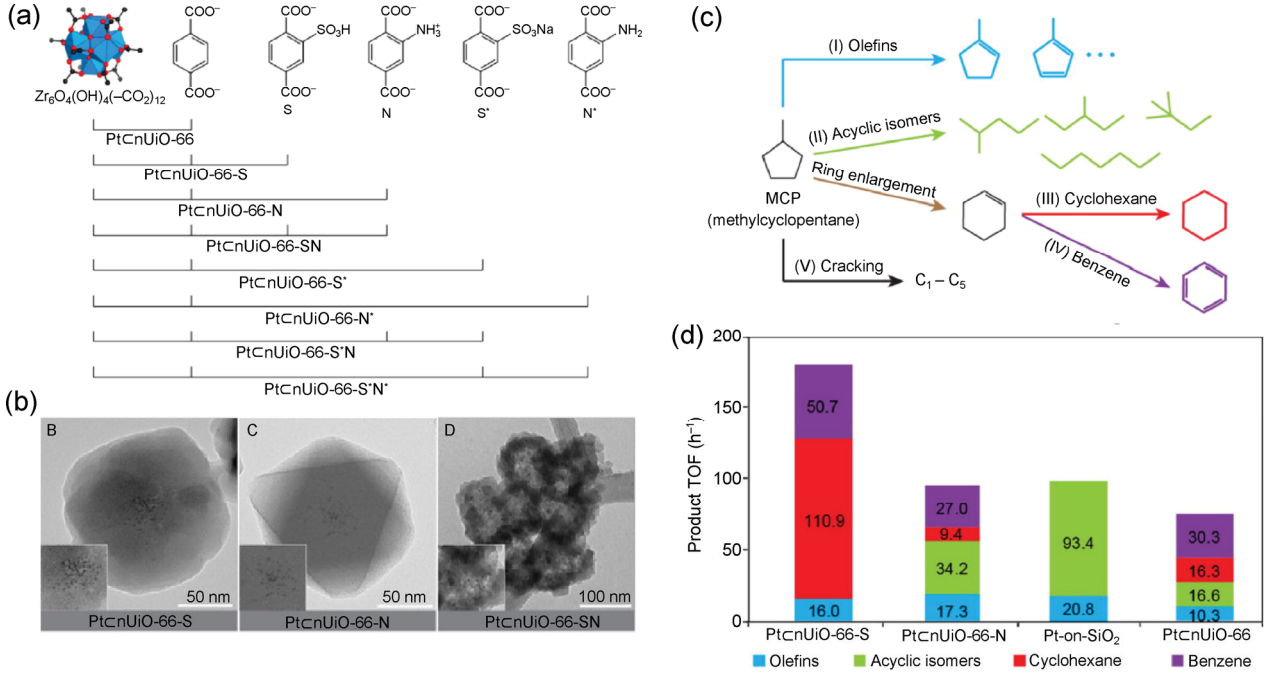

Figure 8 (a) Combination of functionalized linkers used to make nMOFs in the Pt⊂nUiO-66 constructs; (b) TEM images of Pt⊂nUiO-66 constructs; (c) schematic reaction diagram of conversion of MCP; (d) turnover frequency (TOF, h^{-1}) obtained at 150 °C over Pt⊂nUiO-66-S and N, Pt⊂nUiO-66, and Pt-on-SiO_2. (Adapted with permission from Ref. [33], © American Chemical Society 2015.)

of Pt NCs and the strong acidic sites of the sulfonic acid in nUiO-66. Further, the structure, integrity and catalytic performance were preserved after the reaction. The stability together with the tunable MOF structures indicate that MOFs can serve as a platform for heterogeneous catalysis.

Controlling chemical environment on the pore surface is also important for electrochemical energy storage devices such as supercapacitor. During the operation, cations and anions of the electrolyte diffuse through separator into and out of the pores. In this regard, the high porosity and chemical tunablity in MOFs would provide the materials with high capacity storage of ions and robust cycling. In 2014, various nMOFs with different pore size, structures, and organic functionalities were integrated with graphene to provide the materials with tunable pore environment and conductive properties [4]. Through this systematic pore optimization, several members of these materials with high performance were unveiled; in particular, a zirconium MOF with bipyridine linker (nMOF-867) with the stack and areal capacitance of 0.64 F·cm^{-3} and

5.09 mF·cm^{-2}—six times that of commercial activated carbon materials.

4.4 Electron, energy and substrate transfer

Energy transfer is an important mechanism in producing the materials that could harness light and transfer that energy for catalytic applications. Generally, this is achieved by combining two different type of materials that function together but are different. The proximity between these two materials is important for efficient transfer of energy. In this regard, MOFs could function as energy source, which is then transferred to catalytically active sites on metal NCs or vice versa. The developed synthetic methodology to integrate other type of materials together with tunability in MOFs offers spatial control and functionality control to achieve high performance materials.

It has been demonstrated that energy transfer of photo-generated excitons from quantum dots to porphyrin linker can occur in MOFs combining quantum dots and porphyrins as linkers [45]. Typically, organic chromophores or linkers in MOFs have limited region of light absorption, which in turn restricts the photons captured. Combining with quantum dots, which have tunable wavelength of absorption could transfer the energy absorbed to the linker of MOFs via energy transfer process. This energy transfer process broadens the absorption spectrum and hence leads to better utilization of photons of sun spectrum, a key aspect to improve the performance of photoactive materials. Presynthesized CdSe/ZnS core/shell QDs were immobilized on the surface of porphyrin-based MOFs by the coordination between amine and Zn metal on the surface of QDs and MOFs, respectively. By tuning the size of QDs and absorption wavelength of the linkers in the MOFs, the quantum yield of energy transfer as high as 84% has been obtained. The photoluminescence (PL) measurements were also performed to investigate the energy transfer process. DA MOF {Zn_2(DA-Zn)(TCBP), DA-Zn = [5,15-diphenyl-10, 20-bis(pyridin-4-ylethynyl)porphinato]zinc, $TCBP^{4-}$ = 1,2,4,5-tetrakis(4-carboxylatophenyl)benzene} alone shows no PL signal when it is excited at 400 nm (Fig. 9(a)) while QDs immobilized on DA-MOF displays emissions from the QDs and DA-MOF indicating the occurrence of energy transfer (Fig. 9(b)). It should be noted that the spatial arrangement of these two materials are important to achieve such performance which could be controlled by the interactions between those two materials.

The integration of photoactive materials to harvest sunlight and catalysts to utilize the absorbed energy were used to create photocatalytic hydrogen reduction reactions (Fig. 10) [46]. In this case, two Zr-based MOFs functionalized with Ir complex with two different lengths of linkers were used as an absorber. Pt NCs were incorporated into the MOFs by the diffusion of K_2PtCl_4 into the pores followed by TEA mediated photoreduction. Under the irradiation, Ir is excited

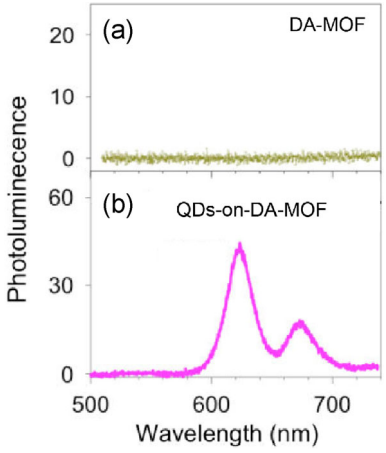

Figure 9 Photoluminescence spectra of DA-MOF (a) showing no PL signal (excitation wavelength = 400 nm). However, the immobilization of QDs on DA-MOF led to the energy transfer from QDs to the MOF as indicated by emissions of DA-MOF (b). (Adapted with permission from Ref. [45], © American Chemical Society 2013.)

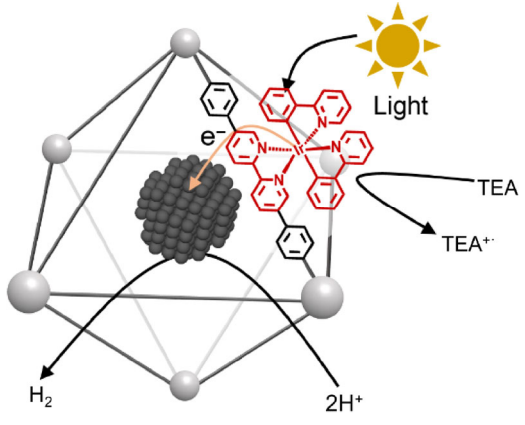

Figure 10 Synergistic photocatalytic hydrogen reduction via photoinjection of electrons from Ir complex in the MOFs into the Pt NCs.

by visible light and subsequently reduced by TEA to generate [$Ir^{III}(ppy)_2(bpy^{\bullet-}$); 2-phenylpyridine; bpy = 2,2′-bipyridine] species. The electrons are then transfered to Pt NCs to catalyze hydrogen reduction reaction. This nanostructure gave a turnover number of 7,000 over 6 h, ca. 5 fold the value obtained in the homogeneous system. The efficient electron transfer from MOFs to Pt NCs and improved stability of the Ir complex due to the rigidity of the frameworks have been ascribed to this enhanced photocatalytic activities.

5 Summary and outlook

In the past few years, tremendous progress in controlling the synthesis of MOFs at the nanoscale has been achieved. With such control over functionalities and variabilities imparted by MOFs, we have progressed to the point where it is possible to design and synthesize materials with precision rarely achieved previously. Given these opportunities, we envisage that the ability to specifically functionalize nanomaterials will lead to a way to code the synergistic interplay occurring at the interface of metal NCs in nMOFs and the synthesis of more complex materials with designed functions.

Acknowledgements

B. R. is supported by the Royal Thai Government Scholarship. Research in the Yaghi group on nanoMOFs is supported by BASF (Ludwigshafen, Germany) and U.S. Department of Defense, Defense Threat Reduction Agency (No. HDTRA 1-12-1-0053). We thank Profs. Gabor Somorjai and Peidong Yang and their research group members for our ongoing collaborations on aspects of this review.

References

[1] Furukawa, H.; Müller, U.; Yaghi, O. M. "Heterogeneity within order" in metal–organic frameworks. *Angew. Chem., Int. Ed.* **2015**, *54*, 3417–3430.

[2] Furukawa, H.; Cordova, K. E.; O'Keeffe, M.; Yaghi, O. M. The chemistry and applications of metal–organic frameworks. *Science* **2013**, *341*, 1230444.

[3] Tanaka, D.; Henke, A.; Albrecht, K.; Moeller, M.; Nakagawa, K.; Kitagawa, S.; Groll, J. Rapid preparation of flexible porous coordination polymer nanocrystals with accelerated guest adsorption kinetics. *Nat. Chem.* **2010**, *2*, 410–416.

[4] Choi, K. M.; Jeong, H. M.; Park, J. H.; Zhang, Y.-B.; Kang, J. K.; Yaghi, O. M. Supercapacitors of nanocrystalline metal–organic frameworks. *ACS Nano* **2014**, *8*, 7451–7457.

[5] Stylianou, K. C.; Imaz, I.; Maspoch, D. Metal–organic frameworks: Nanoscale frameworks. In *Encyclopedia of Inorganic and Bioinorganic Chemistry*; John Wiley & Sons, Ltd.: New York, 2011.

[6] Valtchev, V.; Tosheva, L. Porous nanosized particles: Preparation, properties, and applications. *Chem. Rev.* **2013**, *113*, 6734–6760.

[7] Flügel, E. A.; Ranft, A.; Haase, F.; Lotsch, B. V. Synthetic routes toward MOF nanomorphologies. *J. Mater. Chem.* **2012**, *22*, 10119–10113.

[8] Hermes, S.; Witte, T.; Hikov, T.; Zacher, D.; Bahnmüller, S.; Langstein, G.; Huber, K.; Fischer, R. A. Trapping metal–organic framework nanocrystals: An *in-situ* time-resolved light scattering study on the crystal growth of MOF-5 in solution. *J. Am. Chem. Soc.* **2007**, *129*, 5324–5325.

[9] Tsuruoka, T.; Furukawa, S.; Takashima, Y.; Yoshida, K.; Isoda, S.; Kitagawa, S. Nanoporous nanorods fabricated by coordination modulation and oriented attachment growth. *Angew. Chem., Int. Ed.* **2009**, *48*, 4739–4743.

[10] Umemura, A.; Diring, S.; Furukawa, S.; Uehara, H.; Tsuruoka, T.; Kitagawa, S. Morphology design of porous coordination polymer crystals by coordination modulation. *J. Am. Chem. Soc.* **2011**, *133*, 15506–15513.

[11] Schaate, A.; Roy, P.; Godt, A.; Lippke, J.; Waltz, F.; Wiebcke, M.; Behrens, P. Modulated synthesis of Zr-based metal–organic frameworks: From nano to single crystals. *Chem. Eur. J.* **2011**, *17*, 6643–6651.

[12] Lu, G.; Cui, C. L.; Zhang, W. N.; Liu, Y. Y.; Huo, F. W. Synthesis and self-assembly of monodispersed metal–organic framework microcrystals. *Chem. Asian J.* **2013**, *8*, 69–72.

[13] Wißmann, G.; Schaate, A.; Lilienthal, S.; Bremer, I.; Schneider, A. M.; Behrens, P. Modulated synthesis of Zr-fumarate MOF. *Micropor. Mesopor. Mater.* **2012**, *152*, 64–70.

[14] Cravillon, J.; Nayuk, R.; Springer, S.; Feldhoff, A.; Huber, K.; Wiebcke, M. Controlling zeolitic imidazolate framework nano- and microcrystal formation: Insight into crystal growth by time-resolved *in situ* static light scattering. *Chem. Mater.* **2011**, *23*, 2130–2141.

[15] Liu, Q.; Jin, L.-N.; Sun, W.-Y. Facile fabrication and adsorption property of a nano/microporous coordination polymer with controllable size and morphology. *Chem. Commun.* **2012**, *48*, 8814–8816.

[16] Nune, S. K.; Thallapally, P. K.; Dohnalkova, A.; Wang, C. M.; Liu, J.; Exarhos, G. J. Synthesis and properties of nano zeolitic imidazolate frameworks. *Chem. Commun.* **2010**, *46*, 4878–4880.

[17] Ranft, A.; Betzler, S. B.; Haase, F.; Lotsch, B. V. Additive-mediated size control of MOF nanoparticles. *CrystEngComm* **2013**, *15*, 9296–9300.

[18] Reboul, J.; Furukawa, S.; Horike, N.; Tsotsalas, M.; Hirai, K.; Uehara, H.; Kondo, M.; Louvain, N.; Sakata, O.; Kitagawa, S. Mesoscopic architectures of porous coordination polymers fabricated by pseudomorphic replication. *Nat. Mater.* **2012**, *11*, 717–723.

[19] Zhan, W.-W.; Kuang, Q.; Zhou, J.-Z.; Kong, X.-J.; Xie, Z.-X.; Zheng, L.-S. Semiconductor@metal–organic framework core–shell heterostructures: A case of ZnO@ZIF-8 nanorods with selective photoelectrochemical response. *J. Am. Chem. Soc.* **2013**, *135*, 1926–1933.

[20] Zhao, Y. B.; Kornienko, N.; Liu, Z.; Zhu, C. H.; Asahina, S.; Kuo, T.-R.; Bao, W.; Xie, C. L.; Hexemer, A.; Terasaki, O. et al. Mesoscopic constructs of ordered and oriented metal–organic frameworks on plasmonic silver nanocrystals. *J. Am. Chem. Soc.* **2015**, *137*, 2199–2202.

[21] Li, S. Z.; Huo, F. W. Metal-organic framework composites: From fundamentals to applications. *Nanoscale* **2015**, *7*, 7482–7501.

[22] Hu, P.; Morabito, J. V.; Tsung, C.-K. Core–shell catalysts of metal nanoparticle core and metal–organic framework shell. *ACS Catal.* **2014**, *4*, 4409–4419.

[23] Foo, M. L.; Matsuda, R.; Kitagawa, S. Functional hybrid porous coordination polymers. *Chem. Mater.* **2014**, *26*, 310–322.

[24] Liu, Y. L.; Tang, Z. Y. Multifunctional nanoparticle@MOF core–shell nanostructures. *Adv. Mater.* **2013**, *25*, 5819–5825.

[25] Meilikhov, M.; Yusenko, K.; Esken, D.; Turner, S.; Van Tendeloo, G.; Fischer, R. A. Metals@MOFs—Loading MOFs with metal nanoparticles for hybrid functions. *Eur. J. Inorg. Chem.* **2010**, *2010*, 3701–3714.

[26] Hermes, S.; Schröter, M.-K.; Schmid, R.; Khodeir, L.; Muhler, M.; Tissler, A.; Fischer, R. W.; Fischer, R. A. Metal@MOF: Loading of highly porous coordination polymers host lattices by metal organic chemical vapor deposition. *Angew. Chem., Int. Ed.* **2005**, *44*, 6237–6241.

[27] Hwang, Y. K.; Hong, D.-Y.; Chang, J.-S.; Jhung, S. H.; Seo, Y.-K.; Kim, J.; Vimont, A.; Daturi, M.; Serre, C.; Férey, G. Amine grafting on coordinatively unsaturated metal centers of MOFs: Consequences for catalysis and metal encapsulation. *Angew. Chem., Int. Ed.* **2008**, *47*, 4144–4148.

[28] Chen, L. Y.; Chen, H. R.; Luque, R.; Li, Y. W. Metal–organic framework encapsulated Pd nanoparticles: Towards advanced heterogeneous catalysts. *Chem. Sci.* **2014**, *5*, 3708–3714.

[29] Aijaz, A.; Karkamkar, A.; Choi, Y. J.; Tsumori, N.; Rönnebro, E.; Autrey, T.; Shioyama, H.; Xu, Q. Immobilizing highly catalytically active Pt nanoparticles inside the pores of metal–organic framework: A double solvents approach. *J. Am. Chem. Soc.* **2012**, *134*, 13926–13929.

[30] Zhu, Q.-L.; Li, J.; Xu, Q. Immobilizing metal nanoparticles to metal–organic frameworks with size and location control for optimizing catalytic performance. *J. Am. Chem. Soc.* **2013**, *135*, 10210–10213.

[31] Gu, X. J.; Lu, Z. H.; Jiang, H. L.; Akita, T.; Xu, Q. Synergistic catalysis of metal–organic framework-immobilized Au-Pd nanoparticles in dehydrogenation of formic acid for chemical hydrogen storage. *J. Am. Chem. Soc.* **2011**, *133*, 11822–11825.

[32] Zhou, J. J.; Wang, P.; Wang, C. X.; Goh, Y. T.; Fang, Z.; Messersmith, P. B.; Duan, H. W. Versatile core–shell nanoparticle@metal–organic framework nanohybrids: Exploiting mussel-inspired polydopamine for tailored structural integration. *ACS Nano* **2015**, *9*, 6951–6960.

[33] Choi, K. M.; Na, K.; Somorjai, G. A.; Yaghi, O. M. Chemical environment control and enhanced catalytic performance of platinum nanoparticles embedded in nanocrystalline metal–organic frameworks. *J. Am. Chem. Soc.* **2015**, *137*, 7810–7816.

[34] Zhao, M. T.; Deng, K.; He, L. C.; Liu, Y.; Li, G. D.; Zhao, H. J.; Tang, Z. Y. Core–shell palladium nanoparticle@metal–organic frameworks as multifunctional catalysts for cascade reactions. *J. Am. Chem. Soc.* **2014**, *136*, 1738–1741.

[35] Zhang, W. N.; Lu, G.; Cui, C. L.; Liu, Y. Y.; Li, S. Z.; Yan, W. J.; Xing, C.; Chi, Y. R.; Yang, Y. H.; Huo, F. W. A family of metal–organic frameworks exhibiting size-selective catalysis with encapsulated noble-metal nanoparticles. *Adv. Mater.* **2014**, *26*, 4056–4060.

[36] Na, K.; Choi, K. M.; Yaghi, O. M.; Somorjai, G. A. Metal nanocrystals embedded in single nanocrystals of MOFs give unusual selectivity as heterogeneous catalysts. *Nano Lett.* **2014**, *14*, 5979–5983.

[37] Hu, P.; Zhuang, J.; Chou, L.-Y.; Lee, H. K.; Ling, X. Y.; Chuang, Y.-C.; Tsung, C.-K. Surfactant-directed atomic to mesoscale alignment: Metal nanocrystals encased individually in single-crystalline porous nanostructures. *J. Am. Chem. Soc.* **2014**, *136*, 10561–10564.

[38] He, L. C.; Liu, Y.; Liu, J. Z.; Xiong, Y. S.; Zheng, J. Z.; Liu, Y. L.; Tang, Z. Y. Core–shell noble-metal@metal-organic-framework nanoparticles with highly selective sensing property. *Angew. Chem., Int. Ed.* **2013**, *52*, 3741–3745.

[39] Lu, G.; Li, S. Z.; Guo, Z.; Farha, O. K.; Hauser, B. G.; Qi, X. Y.; Wang, Y.; Wang, X.; Han, S. Y.; Liu, X. G. et al. Imparting functionality to a metal–organic framework material by controlled nanoparticle encapsulation. *Nat. Chem.* **2012**, *4*, 310–316.

[40] Kuo, C. H.; Tang, Y.; Chou, L. Y.; Sneed, B. T.; Brodsky, C. N.; Zhao, Z. P.; Tsung, C. K. Yolk–shell nanocrystal@ZIF-8 nanostructures for gas-phase heterogeneous catalysis with selectivity control. *J. Am. Chem. Soc.* **2012**, *134*, 14345–14348.

[41] Falcaro, P.; Hill, A. J.; Nairn, K. M.; Jasieniak, J.; Mardel, J. I.; Bastow, T. J.; Mayo, S. C.; Gimona, M.; Gomez, D.; Whitfield, H. J. et al. A new method to position and functionalize metal–organic framework crystals. *Nat. Commun.* **2011**, *2*, 237.

[42] Khaletskaya, K.; Reboul, J.; Meilikhov, M.; Nakahama, M.; Diring, S.; Tsujimoto, M.; Isoda, S.; Kim, F.; Kamei, K. I.; Fischer, R. A. et al. Integration of porous coordination polymers and gold nanorods into core–shell mesoscopic composites toward light-induced molecular release. *J. Am. Chem. Soc.* **2013**, *135*, 10998–11005.

[43] Kreno, L. E.; Greeneltch, N. G.; Farha, O. K.; Hupp, J. T.; Van Duyne, R. P. SERS of molecules that do not adsorb on Ag surfaces: A metal–organic framework-based functionalization strategy. *Analyst* **2014**, *139*, 4073–4080.

[44] Sugikawa, K.; Furukawa, Y.; Sada, K. SERS-active metal–organic frameworks embedding gold nanorods. *Chem. Mater.* **2011**, *23*, 3132–3134.

[45] Jin, S. Y.; Son, H. J.; Farha, O. K.; Wiederrecht, G. P.; Hupp, J. T. Energy transfer from quantum dots to metal–organic frameworks for enhanced light harvesting. *J. Am. Chem. Soc.* **2013**, *135*, 955–958.

[46] Wang, C.; deKrafft, K. E.; Lin, W. B. Pt nanoparticles@ photoactive metal–organic frameworks: Efficient hydrogen evolution via synergistic photoexcitation and electron injection. *J. Am. Chem. Soc.* **2012**, *134*, 7211–7214.